Latex Film Formation Probed by Nonradiative Energy Transfer: Effect of Grafted and Free Poly(ethylene oxide) on a Poly(*n*-butyl methacrylate) Latex

J. P S. Farinha and J. M. G. Martinho*

Centro de Química-Física Molecular, Instituto Superior Técnico, Av. Rovisco Pais, 1096 Lisboa Codex, Portugal

Seigou Kawaguchi,† Ahmad Yekta, and Mitchell A. Winnik

Department of Chemistry and Erindale College, University of Toronto, Toronto, Ontario M5S 1A1, Canada

Received: January 24, 1996; In Final Form: April 30, 1996[⊗]

The formation of solid films from latex dispersions is studied using particles labeled with phenanthrene or anthracene comprised of either poly(*n*-butyl methacrylate) (PBMA) or a copolymer of *n*-butyl methacrylate with a poly(ethylene oxide) (PEO) macromonomer, co(PBMA−PEO). Interparticle polymer diffusion was followed by nonradiative electronic energy transfer (DET) between electronically excited phenanthrene and anthracene. A model of energy transfer that considers both the topological constraints and the heterogeneous distributions of donors and acceptors is presented. The analysis of the phenanthrene decay curves allows calculation of the diffusion coefficient as a unique parameter, for several annealing times. The values recovered decrease initially with annealing time, which was attributed mainly to the polydispersity of the PBMA. The addition of a small percentage of low molecular weight PEO (in the form of nonylphenolethoxylate) to the PBMA particles increases the diffusion coefficient, this effect resulting from the increase of the polymer free volume in the film. When the same percentage of PEO is incorporated in the PBMA polymer chain in the form of a grafted macromonomer, the fraction of mixing increases on drying, but during annealing the diffusion coefficients remain equal to that of PBMA without PEO.

1. Introduction

Polymer diffusion across interfaces is a subject which has received increasing attention because of its importance in polymer welding, adhesion, and processing, lamination of composites, polymer blends, and latex film formation. Here we are interested in polymer diffusion leading to the formation of transparent continuous films from a colloidal dispersion of latex particles.

After water evaporation and drying, latex films formed from surfactant free particles have ordered structures corresponding to densely close-packed particle arrangements, as observed by transmission electron microscopy (TEM)[1,2] and by freeze-fracture transmission electron microscopy (FF-TEM).[3,4] After this initial deformation of the particles,[5,6] the mechanical strength of the film is improved by coalescence of the particles which occurs by healing of the interface between them. The healing results from interparticle polymer diffusion occurring above the minimum film formation temperature (MFT), which is close to the glass transition temperature (T_g) of the polymer in the presence of water.

The interdiffusion process in latex films has been followed, at the molecular level, by small angle neutron scattering (SANS) that probes the growth of the radius of deuterium-labeled particles in a protonated matrix as the films are annealed.[7,8] Alternatively, nonradiative electronic energy transfer (DET) has also been used to follow the interdiffusion process using samples which consist of a mixture of donor- and acceptor-labeled particles.[4b,9] Once the donors are electronically excited, they can transfer energy to the acceptors surrounding them, as long as the donor−acceptor distances are of the order of tens of angstroms. At the initial stages, the donors and the acceptors are located in different particles, and nonradiative energy transfer occurs only to a small extent. The annealing of the film at temperatures higher than the MFT promotes the interdiffusion of polymer chains between particles inducing the mixing of donors and acceptors and the consequent increase of the extent of nonradiative energy transfer. The decay curve of the energy donor reflects the increase of the energy transfer processes *via* the distribution functions of donors and acceptors. The analysis of DET in such complex systems requires the development of an energy transfer model that correctly considers the topological constraints of the medium and the heterogeneity of the donor and acceptor distributions.

The donor and acceptor distribution functions result from the mixing that takes place during annealing and can, in principle, be obtained from the analysis of the interparticle diffusion process. The chain dynamics of a polymer with average molecular weight larger than the entanglement molecular weight (M_e) can be described by combining reptation with segmental motion.[10] Usually, depending on the time scale, four regimes can be theoretically predicted:[10−12] At times shorter than the entanglement relaxation time, τ_e, relaxation of segments within the entanglement length occurs. In this case the mean square displacement of the segments is smaller than the tube diameter, and the chains do not sense topological constraints. Between τ_e and the Rouse relaxation time, τ_R, the motion of a single segment becomes coordinated over the entire length of the chain and its dynamics can be described by Rouse-like diffusion constrained inside the tube. Between τ_R and the reptation time, τ_r (the time required for the chain to lose the memory of its original tube), reptation gradually dominates the molecular motion. At longer times ($t > \tau_r$) the chain loses memory of the original tube and continues the reptation in a new tube.

* To whom correspondence should be addressed.
† Permanent address: Department of Materials Science, Toyohashi University of Technology, Tempaku-cho, Toyohashi 441, Japan.
⊗ Abstract published in *Advance ACS Abstracts,* June 15, 1996.

S0022-3654(96)00236-5 CCC: $12.00

Consequently, successive displacements are statistically independent, and the dynamics of the polymer is described by the Fickian motion of its center-of-mass.

The distribution functions of polymer chains at the interface resulting from both reptation and segmental motion are rather complex for $t < \tau_r$.[11,12] For times longer than the reptation time, τ_r, the chain dynamics is described by the diffusion of its center-of-mass, and concentration profiles across the interface are given by the solution of Fick's equations. The mass crossing the interface for $t > \tau_r$ scales as $t^{1/2}$, but for $t < \tau_r$, the precise time dependence is unknown. Nevertheless, a different time dependence is expected, leading to a crossover near the reptation time.[11,12]

In this work we examine interparticle diffusion in latex films of poly(*n*-butyl methacrylate) (PBMA) and of a copolymer of *n*-butyl methacrylate grafted with a poly(ethylene oxide) (PEO) macromonomer, co(PBMA−PEO). The monodisperse latex particles ($d \approx 130$ nm) consist of polydisperse polymer chains ($M_w/M_n \approx 3$), labeled with either phenanthrene (energy donor) or anthracene (energy acceptor) groups attached randomly along the polymer backbone to a small extent (ca. 1 mol %). A model for nonradiative energy transfer that considers both the packing of the particles and the distribution of polymer chains is presented.

Individual latex films were annealed at 90 °C for various periods of time, cooled to room temperature to stop diffusion and for fluorescence measurements to be made, and then reheated to 90 °C. Fitting the experimental energy donor fluorescence decay curves of these films to an appropriate theoretical decay law allows us to determine the corresponding diffusion coefficients. The diffusion coefficients of PBMA in the absence of free PEO decrease with annealing time from the beginning of the experiment until they attain a constant value at longer times. The decrease of the diffusion coefficient at early times is attributed to the polydispersity of the polymer chains. Indeed, at short annealing times, the dominant mode of molecular mixing is due to the smaller chains in the sample that diffuse quickly.[13] At longer times, an homogeneous distribution of these molecules is attained, and only the longer chains contribute to the increase of molecular mixing. The diffusion coefficients of the PBMA and the PBMA with grafted PEO chains are practically equal. On the other hand, addition of unbound PEO to the PBMA particles, in the form of a nonylphenolethoxylate nonionic surfactant, substantially increases the diffusion coefficient of PBMA. This is attributed to the plasticizing properties of the surfactant. The mass transferred across the original interface increases with time, rapidly at first and then more slowly, until attaining a $t^{1/2}$ time dependence. A crossover around 25 min is detected in the plot, which is close to the reptation time of PBMA chains at the annealing temperature of 90 °C.

2. Electronic Energy Transfer in Heterogeneous Mediums

The electronic energy of an excited molecule (the donor) can be transferred to another (the acceptor) if the fluorescence spectrum of the donor overlaps the absorption spectrum of the acceptor. For a dipole−dipole coupling mechanism the rate of energy transfer, $\omega(r)$, between donor and acceptor separated by a distance r, is given by Förster's equation[14]

$$\omega(r) = \alpha/r^6 \tag{1}$$

where

$$\alpha = 3R_0^{\,6}k^2/2\tau_D \tag{2}$$

Here R_0 is the critical Förster distance, τ_D is the intrinsic fluorescence lifetime of the excited donor, and k^2 is a dimensionless parameter related to the relative orientation of the donor and acceptor transition dipoles moments.[15] The decay probability of a donor at position $\mathbf{r}_D$ due to the presence of an acceptor molecule at position $\mathbf{r}_i$ is

$$f(t,\mathbf{r}_D,\mathbf{r}_i) = \exp[-t\omega(|\mathbf{r}_i - \mathbf{r}_D|)] \tag{3}$$

Following the procedures introduced by Blumen, Klafter, and Zumofen[16] and recently developed in our laboratories,[17,18] we will consider that donors and acceptors occupy discrete sites in a restricted space. Assuming that donors and acceptors act independently, the donor decay is given by the product of the donor transition probabilities weighted by the distribution functions, $g(\mathbf{r}_i, j)$, of the number of acceptors, j, in each site, $\mathbf{r}_i$

$$F(t,\mathbf{r}_D) = \prod_{\mathbf{r}_i \neq \mathbf{r}_D} \left\{ \sum_j g(\mathbf{r}_i, j)[f(t,\mathbf{r}_D,\mathbf{r}_i)]^j \right\} \tag{4}$$

If the probability of having one acceptor in $\mathbf{r}_i$ is small, the probability that j acceptors exist in the site $\mathbf{r}_i$ is given by a Poisson distribution with mean equal to the number of acceptors $n_A(\mathbf{r}_i)$

$$g(\mathbf{r}_i, j) = \exp[-n_A(\mathbf{r}_i)] \frac{n_A{}^j(\mathbf{r}_i)}{j!} \tag{5}$$

The decay probability of the donor is thus given by

$$F(t,\mathbf{r}_D) = \prod_{\mathbf{r}_i \neq \mathbf{r}_D} \left\{ \sum_j \exp[-n_A(\mathbf{r}_i)] \frac{n_A{}^j(\mathbf{r}_i)}{j!} f^j(t,\mathbf{r}_D,\mathbf{r}_i) \right\} \tag{6}$$

which can be rewritten as

$$F(t,\mathbf{r}_D) = \exp(-\sum_{\mathbf{r}_i \neq \mathbf{r}_D} n_A(\mathbf{r}_i) \{1 - \exp[-t\omega(|\mathbf{r}_i - \mathbf{r}_D|)]\}) \tag{7}$$

and considering that the donor is inside a continuous restricted space of volume V

$$F(t,\mathbf{r}_D) = \exp(-\int_V C_A(\mathbf{r}_A) \{1 - \exp[-t\omega(|\mathbf{r}_A - \mathbf{r}_D|)]\} \, d\mathbf{r}_A) \tag{8}$$

where the integral is performed over the volume elements $d\mathbf{r}_A$ containing acceptors in concentration $C_A(\mathbf{r}_A)$. Normalizing the concentration of acceptors to its initial value, C_{A0}, we obtain

$$F(t,\mathbf{r}_D) = \exp(-C_{A0}\int_{V_D} g_A(\mathbf{r}_A) \{1 - \exp[-t\omega(|\mathbf{r}_A - \mathbf{r}_D|)]\} \, d\mathbf{r}_A) \tag{9}$$

where $g_A(\mathbf{r}_A) = C_A(\mathbf{r}_A)/C_{A0}$ is the distribution function of acceptors.

Donors located at different positions are surrounded by distinct distributions of acceptors and so decay differently. This requires averaging over all the donors in the system, yielding

$$J(t) = -C_{D0}\int_V g_D(\mathbf{r}_D) \, F(t,\mathbf{r}_D) \, d\mathbf{r}_D \tag{10}$$

where the distribution function of donors $g_D(\mathbf{r}_D) = C_D(\mathbf{r}_D)/C_{D0}$ and C_{D0} is the initial uniform concentration of donors in the donor-labeled phase.

Equations 9 and 10 describe the donor decay due to the electronic energy transfer processes occurring in a confined space where donors and acceptors have a heterogeneous distributions. The geometric restrictions are introduced by the

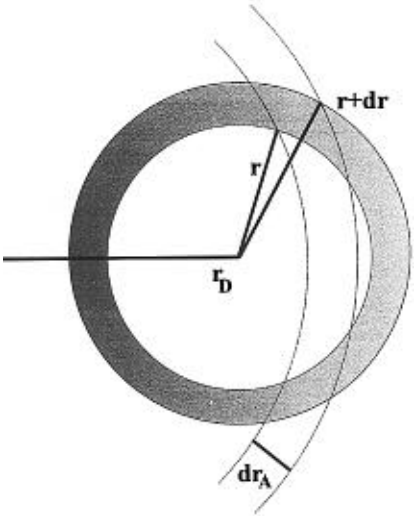

Figure 1. Scheme of the distribution of acceptors surrounding a donor located at $\mathbf{r}_D$. The gray scale in the spherical shell around the donors represents a gradient in acceptor concentration.

volume V over which the integral is calculated and the heterogeneity, by position-dependent donor and acceptor concentrations.

We now consider the particular case of spherical symmetric distribution functions of donors and acceptors. Equation 9 simplifies to

$$F(t,\mathbf{r}_D) = \exp(-C_{A0}\int_{-\pi}^{\pi}\int_{0}^{\pi}\int_{R_e}^{\infty} g_A(r_A)\{1 - \exp[-\omega(r)t]\}\, \boldsymbol{r}^2 \sin\varphi\, dr\, d\varphi\, d\theta) \quad (11)$$

where

$$r_A = |\mathbf{r}_D + \mathbf{r}| = \sqrt{\mathbf{r}^2 + \mathbf{r}^2{}_D + 2\mathbf{r}\mathbf{r}_D \sin\varphi\cos\theta} \quad (12)$$

$\mathbf{r}$ is the donor−acceptor distance vector and R_e is the donor−acceptor encounter distance.

The integration in eq 11 can be further simplified noticing that $g_A(r_A)$ is symmetric relative to the origin, while $\omega(r)$ is symmetric relative to the donor position.[17,18] Then, the product $g_A(r_A) \times \omega(r)$ is invariant in the volume element defined by the interception of one spherical shell centered in the origin with radius r_A and width dr_A, and another centered in the donor position $\mathbf{r}_D$ with radius r and width dr. This volume element defines a ring with cross section as is depicted in Figure 1, and volume

$$dv = 2\pi \frac{r r_A}{r_D} dr\, dr_A \quad (13)$$

The integral has to be evaluated for each donor−acceptor separation r, over all rings at distances $r_D - r$ to $r_D + r$, to obtain an average concentration of acceptors over the rings defining a spherical shell of radius r, centered in the donor position. The resulting expression integrated over all donor−acceptor distances r, yields

$$F(t,\mathbf{r}_D) = \exp\left(-\frac{2\pi}{\mathbf{r}_D} C_{A0}\int_{R_e}^{\infty}\{1 - \exp[-\omega(r)t]\}\,[\int_{r_D-r}^{r_D+r} g_A(r_A) r_A\, dr_A] r\, dr\right) \quad (14)$$

which allows the determination of the donor decay expression from eq 10 in a very convenient way for our system.

Experimental Section

Materials. Nonylphenolethoxylate (NP-20) surfactant, a gift from ICI, was purified by two times reprecipitation from benzene into hexane at −78 °C and then freeze-dried from benzene. Measurements by proton nuclear magnetic ressonance, ^{1}H NMR, and gel permeation cromatography, GPC, yield M_n of the PEO as 20 and M_w/M_n as 1.08, where M_w and M_n are the weight and number averaged molecular weight, respectively. The PEO macromonomer was prepared and characterized by methods reported previously.[19,20]

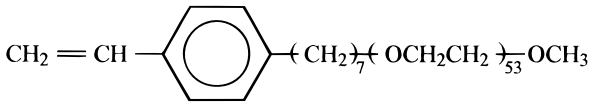

PEO macromonomer

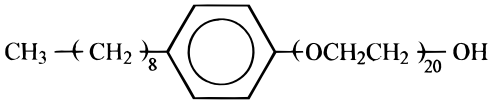

NP-20

n-Butyl methacrylate (BMA, Aldrich) was distilled just before use. Potassium persulfate (KPS), sodium lauryl sulfate (SLS), and sodium bicarbonate (SBC) were used as received. Water was purified by a Millipore Milli Q purification system. α,α′-Azobis(isobutyronitrile) (AIBN) was purified by recrystallization three times from ethanol. 9-Phenanthrylmethacrylate (PheMMA) and 9-anthrylmethacrylate (AnMA) were prepared and used as previously described.[21] Other solvents and chemicals were purified by conventional methods.

Latex Preparation. The anthracene- and phenanthrene-labeled poly(*n*-butyl methacrylate) (PBMA) latex particles were prepared by a two-step semicontinuous polymerization of BMA at 70 °C. The polymerization was carried out under nitrogen in a 50 mL three-neck glass reactor fitted with a condenser and a mechanical stirrer with a half-moon type of impeller rotating at 250 rpm. The additives KPS, SLS, and SBC were used as initiator, emulsifier, and buffer, respectively. The monomer feed rate in the second stage was 1 mL/h and at this stage 1 mol % of PheMMA or AnMA (based on BMA) was added into the reactor as part of the monomer mixture. The details of the procedures for the preparation and characterization of Phe- and An-labeled PBMA latex particles are the same as reported previously.[21] SLS and low molecular weight salts used in the preparation of the latex dispersions were completely removed by an ion exchange resin (Biorad AG501-X8 mixed bed resin).

PBMA latex particles with PEO chains at the surface were prepared by dispersion copolymerization at 70 °C of BMA with the PEO macromonomer (0.97 mol % based upon BMA) in methanol−water media (20 vol % water) with AIBN as an initiator. The reaction solution also contained 1 mol % of PheMMA or AnMA. The details of the preparation were reported before.[19] Complete consumption of PEO macromonomer was confirmed by gel permeation chromatography (GPC) and by ^{1}H NMR. After polymerization, methanol was removed completely from the dispersion by dialysis against deionized water.

Latex Characterization. ^{1}H-NMR spectra were run at room temperature on a Varian Gemini 200 MHz FT NMR spectrometer. Molecular weights were measured by GPC (Waters Ultrastyragel columns, THF as eluent, PMMA and PEO samples as standards for PBMA and PEO materials), fitted with refractive index and fluorescence detectors. Under the experimental conditions used, less than 1 mol % of the total fluorescent

TABLE 1: Characterization of PBMA Latexes

polymer	particle size (d, nm)	M_w	M_w/M_n
Phe-PBMA	121	2.68×10^5	3.34
An-PBMA	117	2.44×10^5	3.43
Phe-co(PBMA−PEO)	132	2.34×10^5	2.73
An-co(PBMA−PEO)	129	2.65×10^5	2.89

monomers remained unattached to the polymer. The diameters of the latex particles were measured by dynamic light scattering (DLS, Brookhaven Instruments, model BI-90 particle sizer with 10 mW He−Ne laser) with a fixed scattering angle of 90°, at 20 °C. The solvent used was spectroscopic grade methanol (Caledon Lab. Ltd.) without further purification (viscosity 0.597 cP). The characterization results of the prepared latex particles are summarized in Table 1.

Film Preparation. Mixtures of phenanthrene- and anthracene-labeled particle dispersions in 1:1 molar ratio were spread onto a quartz plate. The PBMA dispersions, and the PBMA-with-added-NP-20 (PBMA+PEO) dispersions were allowed to dry at a slow evaporation rate (at 36 °C) for about 10 h in order to form transparent films. The latex dispersion of co(PBMA−PEO) particles was dried at 30 °C at a slow evaporation rate, yielding a crack-free, transparent film. The films, supported on quartz plates, were introduced into a quartz tube that was sealed under argon with a rubber septum. The films were annealed at 90 °C for a certain amount of time (from 5 min up to several days), and the fluorescence decay measurements made at 22 °C after each annealing period.

Fluorescence Measurements. The fluorescence decay curves were obtained by the single photon timing technique. The excitation source is a mode-locked Nd:YAG laser (Coherent Model 76-s) whose output frequency (1064 nm) is doubled by a KTP crystal giving pulses of 70 ps full width at half-maximum (fwhm) intensity for a 76 MHz repetition rate. The output beam is used to synchronously pump rhodhamine 6G in a cavity dumped dye laser (Coherent Model 701-3): pulses of about 10 ps fwhm are obtained at 620 nm. This frequency is then doubled with a KTP crystal in order to get UV pulses with a repetition rate of 380 kHz. The dye laser output wavelength of 310 nm was selected by a glass filter. The residual frequency beam reflected in the filter is directed to an Hamamatsu S2840 high-speed PIN silicon photodiode that triggers the stop signal (inverse mode) of the time-to-amplitude converter (TAC). The fluorescence signal, observed at the magic angle to avoid polarization effects, is selected by a single grating monochromator (PTI, 1200 groves/mm, blazed at 500 nm) and viewed by a Hamamatsu R1564U-01 MCP photomultiplier, whose output is used as a start signal for the TAC. The output signals from the TAC are stored in a multichannel analyzer plug-in board in a PC-type computer. Some of the decay curve measurements were done in a conventional single photon timing instrument using as excitation source a gated flash lamp.[22] The instrumental response function was obtained from the light scattered by a concentrated ludox solution in water. All fluorescence measurements of the films in the quartz tubes were carried out at room temperature (22 °C).

The fluorescence decay curves were analyzed on a DEC 2000-300 AXP workstation by an iterative reconvolution method based on the algorithm of Marquardt,[23] in order to determine the best estimates of the fitting parameters.

Fluorescence spectra were recorded on a SPEX Fluorolog 2 spectrofluorometer.

Data and Data Analysis. Latex films formed by drying colloidal dispersions of small monodisperse polymer particles in water are composed of densely close packed particles which deform into space-filling polyhedra.[1−4] Therefore, it is reasonable to consider that a reference donor-labeled particle is surrounded by 12 "first neighbor particles" or "cells" forming a spherical shell (with thickness equal to the diameter of the particle, $2R$) around the reference particle. For a 1:1 mixture of donor- and acceptor-labeled particles, half of the "first neighbors" of the donor-labeled reference particle are, on average, acceptor-labeled particles. These can be considered to occupy half the spherical crown around the reference particle, as shown in Figure 2.

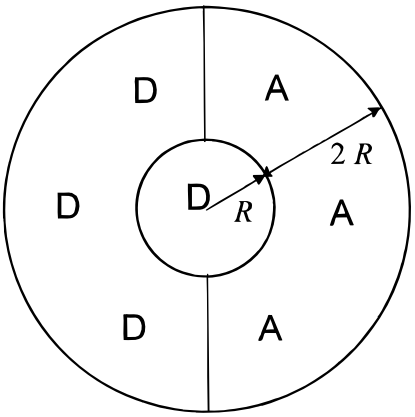

Figure 2. Reference donor labeled particle surrounded by a spherical shell, thickness $2R$, of the neighbouring particles. For a 1:1 ratio of donor to acceptor labeled particles half of the shell is, in average, occupied by acceptor labeled particles

The donor decay law, which now includes the intrinsic deactivation of the donor (with lifetime τ_D), is obtained from eq 10 as

$$J_D(t) = \exp\left(-\frac{t}{\tau_D}\right)[2\pi C_{D0} \int_0^R g_D(\boldsymbol{r}_D)\, F(t,\boldsymbol{r}_D)\boldsymbol{r}_D{}^2\, \mathrm{d}\boldsymbol{r}_D] \quad (15)$$

with $F(t,r_D)$ given by eq 14.

In the fitting procedure, the decay function (eq 15) has to be convoluted with the instrumental response function, $L(t)$, and multiplied by a normalization constant a

$$I_D(\mathrm{t}) = a\, L(t) \otimes J_D(t) \quad (16)$$

The experimental donor decay curves at several annealing times (t_{dif}) were fitted with eq 16 using donor and acceptor distribution function profiles resulting from the spherical Fickian motion of the polymer chains. The donor distribution function after an annealing time t_{dif} is given by [24]

$$g_D(r) = \frac{1}{2}\left[\mathrm{erf}\left(\frac{R+r}{2\sqrt{Dt_{dif}}}\right) + \mathrm{erf}\left(\frac{R-r}{2\sqrt{Dt_{dif}}}\right)\right] + \frac{1}{\mathrm{r}}\sqrt{\frac{Dt_{dif}}{\pi}}\left\{\exp\left(-\frac{(R+r)^2}{4Dt_{dif}}\right) - \exp\left(-\frac{(R-r)^2}{4Dt_{dif}}\right)\right\} \quad (17)$$

where D is the diffusion coefficient of the polymer chains and $\mathrm{erf}(z)$ is the error function. Due to the symmetry of the system (see Figure 2), the acceptor distribution function, $g_A(r)$, can be expressed by

$$g_A(r) = g_D(2R - r) \quad (18)$$

which means that the distribution function of acceptors is centered in the middle of the spherical crown of acceptors. So far, we have only considered the diffusion to and from the "first neighbor" particles, those initially in contact with the reference particle. However, when about 60% of the mass of the reference particle has passed its initial boundary, it is necessary to consider the polymer chains diffusing from "second neighbor" particles.

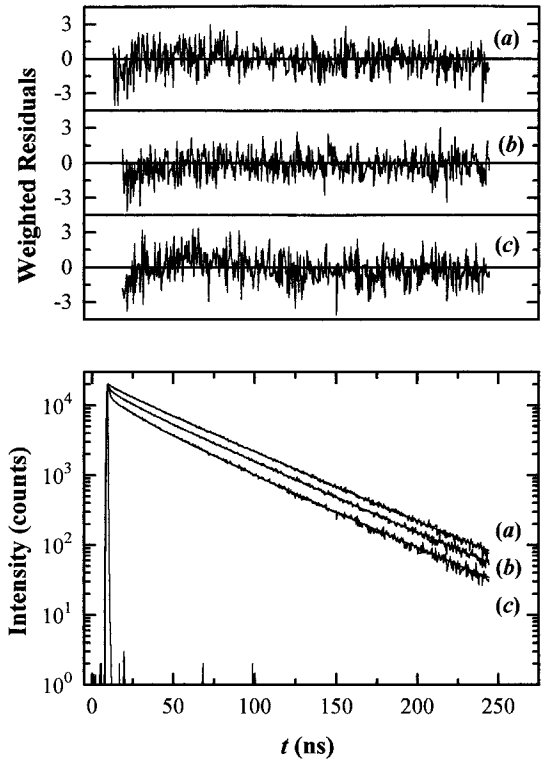

Figure 3. Donor fluorescence decay curves fitted with eq 16 (R_0 = 22.3 Å; τ_D = 44.4 ns) and the respective weighted residuals of a co-(PBMA−PEO) latex film: (a) before annealing; (b) after annealing 300 s at 90 °C; (c) after annealing 5400 s at 90 °C.

These chains can be acceptor- or donor-labeled, and their contribution to the distribution function of polymer chains is very difficult to calculate.

Figure 3 shows the donor decay curves and corresponding residuals for a co(PBMA−PEO) latex film at several annealing times, fitted with eq 16. The decays were fitted with only two parameters: the diffusion coefficient, *D*, and the normalization pre-exponential factor, *a*. The intrinsic donor lifetime, τ_D = 44.4 ns, was obtained from the single exponential decay of a film prepared with phenanthrene-labeled particles which remained constant after successive periods of annealing. The value of the critical transfer distance, R_0 = 22.3 Å, was taken from Wang *et al.*[25] We used a dipole moment orientation factor of $k^2 = 0.476$,[15] which means that the donor and acceptor are randomly oriented and do not rotate during the energy transfer time. The fitting is very good, but only if the analysis begins 3−4 ns after the maximum of the instrumental response function. This is mainly caused by the contamination of the fluorescence decay with a small (but still observable) short lived emission of the quartz plate that supports the films.

Figure 4 shows the plot of the diffusion coefficients obtained at several annealing times for films made of PBMA, PBMA + PEO, and co(PBMA−PEO) particles. These correspond to average values taken over two/three films of each sample and three independent time-correlated single photon timing decay curve measurements, made in two different single photon timing instruments, as described in the Experimental Section.

All the samples show a decrease of the diffusion coefficient with the annealing time, until a plateau is attained. Although for annealing times between the Rouse relaxation time (τ_R) and the reptation time (τ_r) the molecular diffusion of the longer chains is not Fickian,[11] and therefore eq 17 is not completely correct, this decrease is mainly due to the polydispersity of the polymers (see Table 1). At small annealing times the short chains (with molecular weights smaller than the entanglement

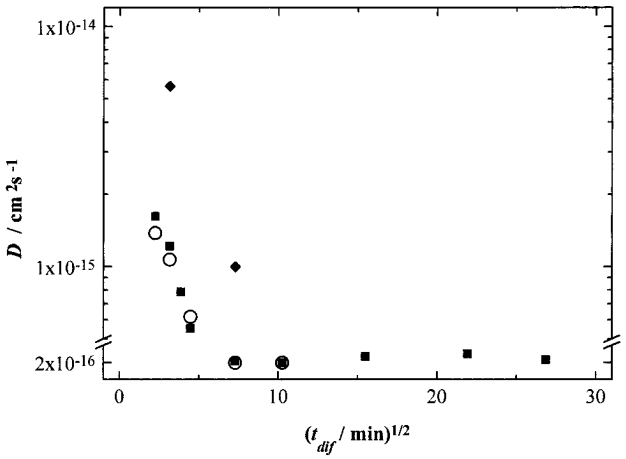

Figure 4. Diffusion coefficients of several latex films versus annealing time at 90 °C (t_{dif}): PBMA (○); co(PBMA−PEO) (□); PBMA plus NP-20 (Δ).

molecular weight of PBMA, M_e = 32 000[25]) diffuse quickly by a Fickian process and are mainly responsible for the initial mixing. Furthermore, at this stage the diffusion coefficients also reflect the contribution of the longer chains' Rouse motion, which allows the chain segments to elbow across the interface with a diffusion coefficient higher than the bulk value.[12] After some time a homogeneous distribution of the short chains is achieved, and afterward only the longer chains contribute to extend the mixing. At this time, the chain dynamics should be dominated by the reptation mechanism which, for times longer than the reptation time, is described by the Fickian motion of the polymer center of mass.

The diffusion coefficients of the PBMA latex polymer are calculated within a polymer diffusion model that does not properly consider complexities of the system resulting from the polydispersity of the PBMA and the change in the diffusion mechanism of the polymer chains with annealing time. Furthermore, our algorithm provides cumulative diffusion coefficients, whose values depend on the previous history of the sample, including the mixing produced on sample drying.

The calculated values obtained here differ from the ones recovered from a previous model of energy transfer (the step function model[4,9,25]) that considered the sample subdivided in three domains: unmixed donors, unmixed acceptors, and homogeneously mixed donors and acceptors in a supposedly infinite medium. The *D* values calculated in this work are lower than the ones obtained by fitting the same data to the step function model (see Table 2). This is a consequence of the formulation of the step-function model, which ignores the distribution functions of donors and acceptors and their time evolution.[17] The recently proposed mean concentration model[26,27] considers a uniform concentration of acceptors surrounding any given donor. The *D* values obtained by this model for similar latex films[27] are closer to our values, with differences observed mainly at early times of annealing, that we attribute to the nonuniformity of the distribution of acceptors around donors.[17] The diffusion coefficients recovered for long annealing times are lower than the ones obtained by SANS for films prepared from latexes of ca. 30 nm radius and similar values of PBMA molecular weight.[7] The radii of these latexes are lower than the radii of gyration of the PBMA chains in their random coil state.[12] This induces conformational changes that act as a driving force for chain diffusion, leading to higher diffusion coefficients than the ones calculated for the two times bigger latexes used in this work.

The diffusion coefficients for both PBMA and co(PBMA−PEO) copolymer are very similar. This shows that a small

TABLE 2: Diffusion Coefficients of PBMA in Latex Particles, Obtained by Different DET Models and SANS[a]

	10^{15} D (cm^2 s^{-1})			
	DET: step function[25]	DET: mean local concentration[26,27]	DET: distribution function (Figure 4)	SANS[7]
t_{dif} (s)	($M_w = 2.2 \times 10^5$; $M_w = 2.6 \times 10^5$)	($M_w = 2.4 \times 10^5$; $M_w = 2.9 \times 10^5$)	($M_w = 2.4 \times 10^5$; $M_w = 2.7 \times 10^5$)	($M_w = 3 \times 10^5$)
180	2.9			
300			1.4	
360		2.1	1.3*	
1200		1.2	0.62	
1440	2.0		0.48*	
1800			0.28*	2.3
2700			0.20*	2.2
3180			0.20	
3240	1.8		0.20*	
3300		0.72	0.20*	
6300			0.20	
7500		0.34	0.20*	
8040	1.5		0.20*	

[a] The values with an asterisk (*) are interpolated from the experimental time evolution of the diffusion coefficient.

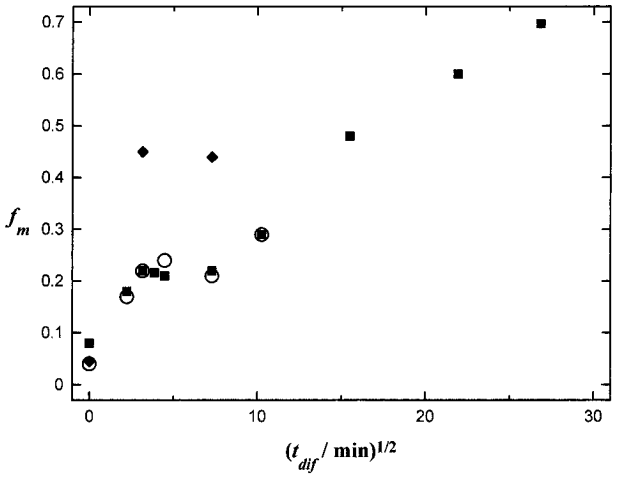

Figure 5. Fraction of mass that crosses the initial interface of the donor-labeled particle versus annealing time at 90 °C (t_{dif}): PBMA (○); co-(PBMA−PEO) (□); PBMA plus NP-20 (Δ).

lateral group attached to the polymer backbone has little influence on the dynamic properties of the chain. The addition of a nonionic surfactant with PEO, NP-20, in the same proportion as the PEO macromonomer in the copolymer, causes a large increase in the diffusion coefficient. This results probably from the plasticizing effect of the NP-20. By increasing the free volume of the system, it acts as a coalescence aid.[28]

Once the diffusion coefficients are known, the mass fraction of mixing can be calculated as

$$f_s = 1 - \frac{1}{\frac{4}{3}\pi R^3} \int_0^\infty 4\pi r^2 g_D(r)\, dr \qquad (19)$$

with $g_D(r)$ given by eq 17. Figure 5 shows the calculated fraction of mixing of the three latex samples for several annealing times, calculated from eq 19.

Since the proposed model takes into account the amount of energy transfer across the interface before annealing, it allows the calculation of the fraction of mixing after drying ($t_{dif} = 0$), which for the PBMA and PBMA + PEO particles are very close to 0.04. On the other hand, the initial fraction of mixing of the co(PBMA−PEO) films is around 0.08, substantially higher than the one calculated for the other particles. This reflects the accumulation of PEO appendages of the co(PBMA−PEO) near the particle surface, which stabilizes the particle in the dispersion and promotes polymer mixing in the films, even at very low temperatures. The PBMA latex films with added NP-20 show a very fast mixing after annealing at 90 °C, due to the plasticizing effect of the surfactant. Both the PEO chains and the end groups contribute to this effect.[29] PBMA and the co-(PBMA−PEO) particles have similar behavior after the initial stage. The fraction of mixing grows very fast at the beginning, appears to show a plateau where little mixing occurs, followed by a steady increase with a $t^{1/2}$ dependence. The initially fast increase of f_s is mainly due to polymer chains with molecular weights lower than the entanglement molecular weight. We suspect that the apparent stationary regime in Figure 5, where there seems to be no mixing, is related to the difficulty of the diffusion model to accommodate the reptation dynamics. In fact, the reptation contribution to the global concentration profile produces less mass mixing than a hypothetical Fickian profile with a constant diffusion coefficient.[30] Therefore, analyzing the results of mixing due to both reptation and Fickian motion with a Fickian model will give smaller apparent diffusion coefficients. This should be detected for annealing times close to the mean reptation time of our PBMA chains which is estimated from $\tau_r = R_g^2/3\pi^2 D$ as 25 min.[12] This is surprisingly close to the annealing time after which f_s scales with $t^{1/2}$, as predicted by the reptation model, for times greater than τ_r.

Conclusions

The process of polymer diffusion in latex films was followed by nonradiative energy transfer experiments. A model of energy transfer that considers both the topological constraints and the heterogeneity in the donor and acceptor concentration profiles was developed. The donor decay curves for these PBMA latex films are well fitted with the model decay function, allowing the calculation of the cumulative (average) diffusion coefficient as the unique transport parameter. These average diffusion coefficients decrease with the annealing time until they attain a plateau at longer times. This time is on the order of the reptation time of polymers with that value of M_w. The initial decrease is mainly attributed to the contribution to mixing of the short chains in the sample. For longer times, the diffusion coefficients should reflect the reptation dynamics of the higher molecular weight chains.

The addition of a small percentage of free PEO (in the form of a nonionic surfactant) increases the diffusion coefficients of the PBMA, due to the plasticizing properties of the additive. On the other hand, when PEO in the same amount, is grafted

at the surface to the PBMA chains, the behavior is very different. The surface PEO chains promote mixing and interdiffusion during the drying process but have little effect on the diffusion coefficient values compared to PBMA latex films, for subsequent annealing of the samples.

Acknowledgment. The authors thank JNICT-PRAXIS XXI/2/2.1/QUI/240/94, the Glidden Co., ICI Canada, and NSERC Canada for their support of this research. J. M. G. Martinho and J. P. S. Farinha thank the Ontario Centre for Materials Research and INVOTAN for support of their stay in Toronto.

References and Notes

(1) Vanderhoff, J. W. *Br. Polym. J.* **1970**, *2*, 161.
(2) (a) Kanig, G.; Neff, H. *Colloid Polym. Sci.* **1975**, *253*, 29. (b) Distler, D.; Kanig, G. *Colloid Polym. Sci.* **1978**, *256*, 1052.
(3) Roulstone, B. J.; Wilkinson, M. C.; Hearn, J.; Wilson, A. J. *Polym. Int.* **1991**, *24*, 87.
(4) (a) Wang, Y.; Kats, A.; Juhué, D.; Winnik, M. A.; Shivers, R. R.; Dinsdale, C. J. *Langmuir* **1992**, *8*, 1435. (b) Wang, Y.; Winnik, M. A. *J. Phys. Chem.* **1993**, *97*, 2507.
(5) Eckersley, S. T.; Rudin, A. *J. Paint Technol.* **1990**, *62*, 89.
(6) (a) Joanicot, M.; Wong, K.; Marquet, J.; Chevalier, Y.; Pichot, C.; Graillat, C.; Lindner, P.; Rios, L; Cabane, B. *Prog. Colloid Polym. Sci.* **1990**, *81*, 157. (b) Chevalier, Y.; Pichot, C.; Graillat, C.; Janicot, M.; Wong, K.; Lindner, P.; Cabane, B. *Colloid Polym. Sci.* **1992**, *270*, 806.
(7) Hahn, K.; Ley, G.; Schuller, H.; Oberthur, R. *Colloid Polym. Sci.* **1986**, *264***,** 1029; **1988**, *266*, 631.
(8) (a) Linne, M. A.; Klein, A.; Sperling, L. H. *J. Macromol. Sci. Phys.* **1988**, *B27*, 181, 217. (b) Yoo, J. N.; Sperling, L. H.; Glinka, C. J.; Klein, A. *Macromolecules* **1990**, *23*, 3962.
(9) (a) Pekan, O.; Winnik, M. A.; Croucher, M. D. *Macromolecules* **1990**, *23*, 2673. (b) Wang, Y.; Winnik, M. A.; Haley, F. *J. Coat. Technol.* **1992**, *64*(811), 51.
(10) Eduards, S. F.; Doi, M. *The Theory of Polymer Dynamics*; Oxford University Press: Oxford, 1988.
(11) (a) Zhang, H.; Wool, R. P. *Polym. Prepr.* **1990**, *2*, 511. (b) Zhang, H.; Wool, R. P. *Macromolecules* **1989**, *22*, 3018.
(12) Wool, R. P. *Polymer Interfaces: Structure and Strength*; Carl Hanser Verlag: Munich, 1995.
(13) Prager, S.; Adolf, D.; Tirell, M. *J. Chem. Phys.* **1983**, *78*, 7015.
(14) Förster, Th. *Ann. Phys.* **1948**, *2*, 55; *Z. Naturforsch.* **1949**, *4A*, 321.
(15) a) Maksimov, M. Z.; Rozman I. M. *Opt. Spectrosc.* **1962**, *12*, 337. (b) Steinberg, I. Z. *J. Chem. Phys.* **1968**, *48*, 2411.
(16) (a) Blumen, A.; Klafter, J.; Zumofen, G. *J. Chem. Phys.* **1986**, *84*, 1397. (b) Klafter, J.; Blumen, A. *J. Chem. Phys.* **1984**, *80*, 875; *J. Lumin.* **1985**, *34*, 77.
(17) Farinha, J. P. S.; Martinho, J. M. G.; Yekta, A.; Winnik, M. A. *Macromolecules* **1995**, *28*, 6084.
(18) Yekta, A.; Duhamel, J.; Winnik, M. A. *Chem. Phys. Lett.* **1995**, *235*, 119.
(19) Kawaguchi, S.; Winnik, M. A.; Ito, K. *Macromolecules* **1995**, *28*, 1159.
(20) Chao, D.; Itsuno, S.; Ito, K. *Polym. J.* **1991**, *23*, 1045.
(21) Zhao, C. L.; Wang, Y.; Hruska, Z.; Winnik, M. A. *Macromolecules* **1990**, *23*, 4082.
(22) Martinho, J. M. G.; Egan, L. S.; Winnik, M. A. *Anal. Chem.* **1987**, *59*, 861.
(23) Marquardt, D. W. *J. Soc. Ind. Appl. Math.* **1963**, *11*, 431.
(24) Crank, J. *The Mathematics of Diffusion*; Clarendon: Oxford, 1975.
(25) Wang, Y.; Zhao, C.-L.; Winnik, M. A. *J. Chem. Phys.* **1991**, *95*, 2143.
(26) Dhinojwala, A.; Torkelson, J. M. *Macromolecules* **1994**, *27*, 4817.
(27) Liu, Y. S.; Feng, J.; Winnik, M. A. *J. Chem. Phys.* **1994**, *101*, 9096.
(28) (a) Juhué, D.; Wang, Y.; Winnik, M. A.; Haley, F. *Makromol. Chem., Rapid Commun.* **1993**, *14*, 345. (b) Wang, Y.; Winnik, M. A. *Macromolecules* **1990**, *23*, 4731.
(29) Karim, A.; Felcher, G. P.; Russel, T. P. *Macromolecules* **1994**, *27*, 6979.

JP960236I